Journal of Digital Imaging (2023) 36:1877–1884
https://doi.org/10.1007/s10278-023-00816-x

# Pilot Lightweight Denoising Algorithm for Multiple Sclerosis on Spine MRI

**John D. Mayfield[1] · Katie Bailey[2] · Andrew A. Borkowski[3] · Narayan Viswanadhan[2]**

Received: 14 September 2022 / Revised: 11 March 2023 / Accepted: 13 March 2023 / Published online: 17 April 2023
© The Author(s) under exclusive licence to Society for Imaging Informatics in Medicine 2023

## Abstract

Multiple sclerosis (MS) is a severely debilitating disease which requires accurate and timely diagnosis. MRI is the primary diagnostic vehicle; however, it is susceptible to noise and artifact which can limit diagnostic accuracy. A myriad of denoising algorithms have been developed over the years for medical imaging yet the models continue to become more complex. We developed a lightweight algorithm which utilizes the image's inherent noise via dictionary learning to improve image quality without high computational complexity or pretraining through a process known as orthogonal matching pursuit (OMP). Our algorithm is compared to existing traditional denoising algorithms to evaluate performance on real noise that would commonly be encountered in a clinical setting. Fifty patients with a history of MS who received 1.5 T MRI of the spine between the years of 2018 and 2022 were retrospectively identified in accordance with local IRB policies. Native resolution 5 mm sagittal images were selected from T2 weighted sequences for evaluation using various denoising techniques including our proposed OMP denoising algorithm. Peak signal to noise ratio (PSNR) and structural similarity index (SSIM) were measured. While wavelet denoising demonstrated an expected higher PSNR than other models, its SSIM was variable and consistently underperformed its comparators ($0.94 \pm 0.10$). Our pilot OMP denoising algorithm provided superior performance with greater consistency in terms of SSIM ($0.99 \pm 0.01$) with similar PSNR to non-local means filtering (NLM), both of which were superior to other comparators (OMP $37.6 \pm 2.2$, NLM $38.0 \pm 1.8$). The superior performance of our OMP denoising algorithm in comparison to traditional models is promising for clinical utility. Given its individualized and lightweight approach, implementation into PACS may be more easily incorporated. It is our hope that this technology will provide improved diagnostic accuracy and workflow optimization for Neurologists and Radiologists, as well as improved patient outcomes.

**Keywords** Multiple sclerosis (MS) · MRI · Denoising · Computer vision · Sparse representation · Orthogonal matching pursuit (OMP)

## Introduction

Multiple sclerosis (MS) is a serious and often fatal autoimmune demyelinating disease which effects patients and formative years of their lives, often while building a family or developing their careers [1, 2]. It is estimated that MS impacted approximately 2.8 million individuals in 2020 [1], a troubling diagnosis as it is typically during the stage of a patient's life when they may be developing a family or the next step in their career. The diagnosis of MS depends on the clinical symptomatology but also the imaging findings suggestive of demyelination in the central nervous system (CNS) where patients often deteriorate with varying degrees of disability [1–3]. Treatment involves immunosuppression which has deleterious consequences and may not always be effective in certain populations. As such, accurate and timely diagnosis are paramount to patients' well-being as well as their future treatment and life planning [1–4]. To this end, magnetic resonance imaging (MRI) is the primary vehicle of radiologic diagnosis for these patients [3, 4, 7–10]. For neurologist and neuroimmunologists, the modification of the existing McDonald criteria from the 2010 version to the 2017 version provided an enhanced role of MRI to provide early diagnosis of MS [3, 4]. Unfortunately, noise in MRI images can mislead diagnosis of subtle MS lesions which may be as small as 3 mm [4–6]. Artifact

✉ John D. Mayfield
jdmayfield@usf.edu

[1] USF Health Department of Radiology, 2 Tampa General Circle, STC 6103, 33612 Tampa, FL, USA

[2] Department of Radiology, James A. Haley VA Medical Center, Tampa, FL, USA

[3] Artificial Intelligence Service, AI Center Lead, USF Morsani College of Medicine, National Artificial Intelligence Institute, James A. Haley Veterans' Hospital, Tampa, FL, USA

is considered a general term which incorporates inherent and extrinsic aberrations in the resultant image which includes noise, a signal that is additive to the patient's anatomic scan and may be due to the MRI, the coil, the patient's clothing, or the postprocessing steps. Inherent noise such as Gaussian, thermal, and Rician noise as well as motion artifact can produce perceived increased signal most noticeable in the spinal cord given its smaller relative diameter compared to intracranial structures [5]. This is an important point as spinal lesions are more specific for MS diagnosis than intracranial lesions [4]; therefore, denoising algorithms have the potential to provide improved diagnostic accuracy and resultant planning.

## Related Works

### MRI Denoising

Denoising techniques have continued to evolve from domain space filters to modern deep learning algorithms [11–14]. Spatial domain filters such as Gaussian blur [15], non-local means filtering (NLM) [16, 17], median filters, et cetera provide a low computational cost, but at the expense of signal to noise ratio resulting in a decrease in diagnostic quality of images. Domain transform filters, such as wavelet transform denoising [18] can be beneficial in maintaining spatial resolution in MRI; however, there needs to be an existing knowledge of the noise present in the image. Combinations of these filters known as fast bilateral filters [19] can maintain edge features and can serve as a viable solution. Linear time-invariant filters such as Weiner filters [20] can provide suitable, low-cost denoising based upon a stochastic noise and signal estimations. Recent studies have demonstrated that single value decomposition (SVD) algorithms can provide benefit in simulated noise removal for MR images whereas spatially adaptive NLM filters provided superior structural similarity to original noisy images [11, 14, 16, 21]. With the technological progression of deep learning models, several studies have shown the superior denoising performance of pretrained CNNs such as ResNet (Residual Network), autoencoders, and generative models [22–26].

While these algorithms have demonstrated objective improvement in medical image quality, there are also several drawbacks that make clinical implementation difficult [22]. The majority of literature involving traditional filtering methods (no deep learning) used simulated noise which can be rather uniform in distribution, unlike real noise created by the patient or scanner. Deep learning models have significant drawbacks to practical use as (1) they must be pretrained, (2) the computational complexity can be an obstacle for fast utilization in a global capacity, and (3) inherent bias can be introduced to these models based upon the training population.

We seek to provide a fast, efficient denoising algorithm that is readily deployable without significant hardware or software requirements based upon sparse representation theory.

### Sparse Representation

Sparse representation in computer vision has continued to develop as an emerging technology based upon classical mathematical theories [27–29]. The driving concept is that a small representative matrix consisting of limited data points can be used to reconstruct an image, thus removing unnecessary information such as noise. These techniques have been used in various fields including security surveillance and national intelligence as well as image compression technology. More specifically, these algorithms provide a way to separate texture versus non-texture surfaces using what is known as a greedy pursuit algorithm, a broad category of optimization algorithms to provide the least number of building blocks necessary to recreate a signal. Similar in purpose to stochastic gradient descent algorithms in machine learning, matching pursuit seeks to minimize the error of recreating the base image from an overcomplete dictionary, a list of multiple vectors either taken from a signal distribution such as discrete cosine transform, or DCT, or an inherent distribution from the noisy image itself. Orthogonal matching pursuit (OMP) requires the sparsest of solutions, in other words the least number of building blocks, in order to reconstruct the denoised original image. There have been a handful of studies [30–35] which have used dictionary learning or sparse representation models in conjunction with deep learning architectures; however, none of these studies utilized solely OMP as a lightweight denoising algorithm.

These preeminent works provided motivation for the algorithm given its performance not only in other fields, however its promise of providing the basic building blocks of an image in an environment of low computational complexity. We feel that this is a significant innovation point in which we are able to provide an individualized denoising algorithm without significant hardware or software investment that can provide improved diagnostic accuracy, clinical workflow, and hopefully, patient outcomes.

**Organization** of the rest of the paper is as such: The "Methods" section will provide insight into the proposed algorithm. Sections titled "Experiment Setup" will describe how the images were denoised and their comparators to traditional denoising algorithms. The "Results" section will elucidate the findings and demonstrate qualitative comparisons. Finally, the "Discussion" section will provide discourse on the impact of the findings with a final synopsis in the "Conclusion" section.

## Methods

### Objective

The primary objective of the study was to develop a lightweight denoising algorithm that would learn noise inherent to the input image and use this overcomplete dictionary of noisy patches in order to create A resultant denoised image

with improved clarity, and specific to clinical application, improved visualization of lesions or dissolution of artifact. Comparison to previously identified domain filtering and transform algorithms was then performed on the same noisy image with resultant peak signal to noise ratio (PSNR) and structural similarity index (SSIM) reported to provide comparison of denoising and edge preservation.

Performance comparison was made to Gaussian blur, NLM filtering, Wavelet denoising, Bilateral filtering, and Weiner filtering. Gaussian blur is of the lowest complexity and simply iterates a kernel over the image with an implied Gaussian distribution of noise. NLM filtering is a form of Low Rank Approximation (LRA) which uses a weighted nuclear norm minimization (WNNM) using spatial Gaussian weighting, usually providing greater edge preservation. Fast NLM was utilized to optimize computation time where sigma (expected noise distribution) was not provided based upon studies demonstrating minimal PSNR increase at the cost of computational time. In contrast, wavelet transformation computed the estimated noise distribution and utilized the BayesShrink algorithm which assigns and individualized soft thresholding for each wavelet representation. Bilateral filtering involves the use of a normalization factor applied to the summation of an image's space and range weights, in other words the impact of a pixel neighborhood and its edges' minimum amplitudes, theoretically resulting in improved edge preservation. Finally, Weiner filtering using linear time-invariant (LTI) filtering in order to determine the transfer function of the image given a stationary noise, similar to a sinusoidal frequency filter.

## Algorithm Architecture

**Dictionary Learning** was chosen over a generic DCT overcomplete dictionary to provide individualized denoising that is unique to the image. To create the dictionary, the noisy image was deconstructed into 8 × 8 overlapping, noisy patches. Least angle regression method (LARS) was used to develop an ideal dictionary based upon the noisy patches which solves for the lasso problem with the optimization objective over 500 iterations such that:

$$min\frac{1}{2n}\|y - Dw\|_2^2 + \alpha\|w\|_1$$

where $n$ is the number of samples, $y$ is the original noisy image, $D$ is a dictionary which is learned from the given reference patches, $w$ is the projected noiseless image, and $\alpha$ is a sparsity-inducing penalty term for the $\updownarrow_1$ norm. This process produces an overcomplete dictionary (Fig. 1) that is used to sparsify the representations.

n_dict_elements to extract = 100;
alpha = 1;
iterations = 500;
batches = 3;
transformation = "Orthogonal Matching Pursuit";
**for** $i$ patches:
  **Input:** noisy patch **y**, Dictionary **A**, Support **S**
  **Initialize:** $k = 0,\ \hat{x}_0 = \mathbf{0},\ \boldsymbol{r}_0 = \boldsymbol{b} - \boldsymbol{A}x_0,\ \mathbf{S}_0 = \emptyset$;
  **for** $k = k + 1$:
    **compute:** $\boldsymbol{E}(i) = \min_z \|za_i - r_{k-1}\|_2^2\ , 1 \le i \le m$;
    **select** $i_0$ s.t. $\forall\ 1 \le i \le m,\ \mathbf{E}(i_0) \le \mathbf{E}(i)$ where $i_0 = argmax\left|A_j^T r^i\right|$;
    **update** $\boldsymbol{S_k}$: $\boldsymbol{S_k} = \boldsymbol{S_{k-1}} \cup \{i_0\}$;
    $\hat{x}_k = \min_x \|A\boldsymbol{x} - \boldsymbol{b}\|_2^2$ s.t. Supp{x} = $S_k$;
    **update** $\boldsymbol{r_k}$: $\boldsymbol{r_k} = \boldsymbol{b} - A\boldsymbol{x_k}$;
  **if** $\|\boldsymbol{r_k}\|_2 \le \boldsymbol{\epsilon}$:
    **stop;**
  **else:**
    $k = k + 1$;
**for** patches:
  Fit to extracted patches by minimization of LASSO problem via LARS:
    $\mathbf{Z} = \min_w \frac{1}{2N}\|y - Xw\|_2^2 + \alpha\|w\|_1$;

**Orthogonal Matching Pursuit (OMP)** was selected to denoise the patches in order to impose the sparsest solution, wherein each row of the original image patch is compared to the corresponding dictionary column and only the correlating, sparse atoms are kept as a projection of the denoised image. Images were subsequently reconstructed using the learned dictionary via OMP such that

$$\alpha = argmin_{\alpha}\|\alpha\|_0^0 s.t. \frac{1}{2}\|D\alpha - y\|_2^2 \leq \epsilon^2$$

where the dictionary is updated column-by-column.

### Implementation

Native T2-weighted sequence image resolution of 256 × 256-pixel slices from was maintained and saved as JPEG format from the DICOM files. Select 4 mm slices with the lesion in question were isolated for denoising. Two dimensional (2D) images were used as the current libraries limit SVD in 3D matrices. As the above, a separate dictionary was created beforehand to use as the overcomplete dictionary required for OMP favored over a generic DCT or equivalent dictionary which would not be specific to the images noise.

**Initialize:** noisy image **Y**, learned dictionary **D**, number of training iterations **j**, Lagrange multiplier $\lambda$;
Extract patches;
**Initialize:** n_nonzero_coefficients = ℕ, reconstructions = ∅, set **X** = **Y**;
**for** $i$ patches:
**Input:** noisy patch **y**, Learned Dictionary **D**, Support **S**;
**Initialize:** $i = 0, j = 0,\ \hat{x}_0 = \mathbf{0},\ \boldsymbol{r}_0 = \boldsymbol{b} - Dx_0,\ \mathbf{S}_0 = \emptyset$;
**for** $\forall_{ij}$:
**compute:** $\min_{\alpha_{ij}} \lambda\|\boldsymbol{Y} - \boldsymbol{X}\| + \sum_{ij}\mu_{ij}\left\|\alpha_{ij}\right\|_{\mathbf{0}} + \sum_{ij}\left\|\boldsymbol{D}\alpha_{ij} - \boldsymbol{R}_{ij}\boldsymbol{X}\right\|_2^2$
**set:** $\boldsymbol{E}_{\ell} = \left\{e_{ij}^{\ell}\right\}_{(i,j)\,\in\,\mathrm{w}_{\ell}}$;
**apply:** SVD decomposition $\boldsymbol{E}_{\ell} = \mathbf{U}\Delta\mathbf{V}^{\mathrm{T}}$;
**update:** columns of **U** with updated dictionary column $\bar{d}_{\ell}$;
**update:** coefficient values $\left\{\alpha_{ij}(\ell)\right\}_{\{i,j\}\in w_{\ell}}$ for values of **V** multiplied by Δ(1,1);

**Denoised Patch Reconstruction** recreates a denoised image to the original resolution without overlap, as such:

**Update** patches:
$\mathbf{E}_{\ell} \cdot \mathbf{Z}$;
**Reconstruct denoised image:**
reconstructions = $\boldsymbol{X} = \left(\lambda I + \sum_{ij}(\boldsymbol{R}_{ij}^{T}\boldsymbol{R}_{ij}\right)^{-1}(\boldsymbol{\lambda Y} + \sum_{ij}\boldsymbol{R}_{ij}^{T}\boldsymbol{D}\alpha_{ij})$;

## Experiment Setup

### Patient Datasets

Fifty patients with a history of MS who underwent an MRI of the spine between the years 2018 and 2021 and whose scans demonstrated noise or artifact as reported by the Neuroradiologists were identified retrospectively in accordance with local IRB protocols. No patient was excluded based upon demographic or background; however, all patients identified were female, not by selection but by availability. Images were captured using a Toshiba 1.5 T and Siemens 1.5 T MRI scanners. Anterior and posterior head coils were combined with the table coils to provide 4 to 5 channels based upon patient size.

In other words, this provides some pre-existing knowledge of the noise to optimize the denoising algorithm. As part of the overcomplete dictionary process, least angle regression (LARS) is used to identify salient features from each noisy patch in order to create the dictionary. Following OMP as described above, the denoised patches are then reconstructed without overlap or compression in order to recreate the original resolution of 256 × 256.

## Results

### Analysis of Denoised Images and Similarity

Similar to findings in the literature review, Wavelet denoising demonstrated superior PSNR compared to other

**Fig. 1** Representative display of an overcomplete dictionary from noisy patches. A matrix of vectors with more representative columns than rows is created using a modified least angle regression algorithm (LARS) which serves as an individualized "noise map" for the subsequent Orthogonal Matching Pursuit (OMP) denoising algorithm

traditional filtering mechanisms but with lower, inconsistent SSIM ($0.94 \pm 0.01$) which was similar to Gaussian Blur ($0.94 \pm 0.02$); however, OMP denoising maintained significantly improved SSIM over all algorithms ($0.99 \pm 0.01$). Both NLM and OMP demonstrated increased PSNR in comparison to the other algorithms with the former demonstrating a non-significant increase in PSNR over OMP ($p = 0.464$). Samples of the denoising algorithms are shown with two cases of suspected artifact and two cases of suspected lesions (Fig. 2) with their respective performances (Table 1).

## Discussion

Comparison to previous studies demonstrated superior performance of the OMP denoising algorithm in terms of denoising and similarity to the original image in terms of edge preservation. While the NLM algorithm demonstrated previously documented edge preservation and thus improved SSIM, OMP denoising provided greater edge preservation and general semblance to the original image. This is an important quantitative aspect to consider in MRI which has inherently lower contrast resolution than CT (Table 1).

As expected, Gaussian blur demonstrated the lowest performance as it is a low complexity filter assuming a normal distribution of noise. Wavelet transformation demonstrated expected superior PSNR, however, many images lost edge detail resulting in a wide variation in SSIM, often well below the OMP algorithm. Bilateral and Wiener filters demonstrated improved edge preservation as expected with the bilateral filter extracting slightly more noise than its counterpart (Table 2).

OMP denoising demonstrates a lean, individualized denoising algorithm that does not require pretraining. Wavelet denoising was the only traditional comparator that consistently outperformed OMP in PSNR but with much lower SSIM. Spatial resolution is already limited in MRI in comparison to CT, therefore, any loss of fine detail may impact diagnostic potential of the image despite increased pixel quality.

The OMP algorithm's performance in comparison to more advanced deep learning models was beyond the scope of this study. These convolutional and generative advanced models may outperform OMP; however, the computational cost and setup are significantly higher. Given the lightweight nature of the OMP denoising algorithm, it could be readily deployed within a Docker container which may be able to integrate easily with PACS versus existing as an inlaid sequence or filter within the Imaging Enterprise system.

Given these benefits, there are still several limitations to this algorithm. Despite the improved SSIM, there is still a perceived generalized blurring that occurs with the denoised image that was readily identified by the neuroradiologists in the study. An additional technical limitation is the current ability of these image processing libraries to evaluate only two-dimensional images and matrices. Further evaluation with 3D models and volumes may provide greater translation to medical imaging which is typically volumetric in nature. Additionally, this small cohort of patients from a single institution may not demonstrate the full potential of the algorithm's ability to denoise images. Further evaluation with the larger cohort is warranted.

**Table 1** Performance comparison of Fig. 2 examples

| | Gaussian blur (k = 3) | | Nonlocal means | | Wavelet ($\sigma = 0.1$) | | Bilateral diffusion | | Weiner filtering | | OMP denoise | |
|---|---|---|---|---|---|---|---|---|---|---|---|---|
| | **PSNR** | **SSIM** | **PSNR** | **SSIM** | **PSNR** | **SSIM** | **PSNR** | **SSIM** | **PSNR** | **SSIM** | **PSNR** | **SSIM** |
| Artifact 1 | 31.8 | 0.93 | 37.7 | 0.97 | 62.7 | 0.95 | 33.8 | 0.92 | 35.3 | 0.96 | 38.3 | 0.99 |
| Artifact 2 | 27.3 | 0.89 | 35.5 | 0.93 | 46.7 | 0.99 | 38.7 | 0.88 | 30.7 | 0.91 | 34.8 | 0.98 |
| Lesion 1 | 33.6 | 0.94 | 38.1 | 0.95 | 57.4 | 0.78 | 34.5 | 0.89 | 35.6 | 0.96 | 38.8 | 0.99 |
| Lesion 2 | 30.6 | 0.96 | 40.8 | 0.98 | 53.7 | 0.98 | 35.0 | 0.96 | 35.0 | 0.97 | 38.3 | 0.99 |

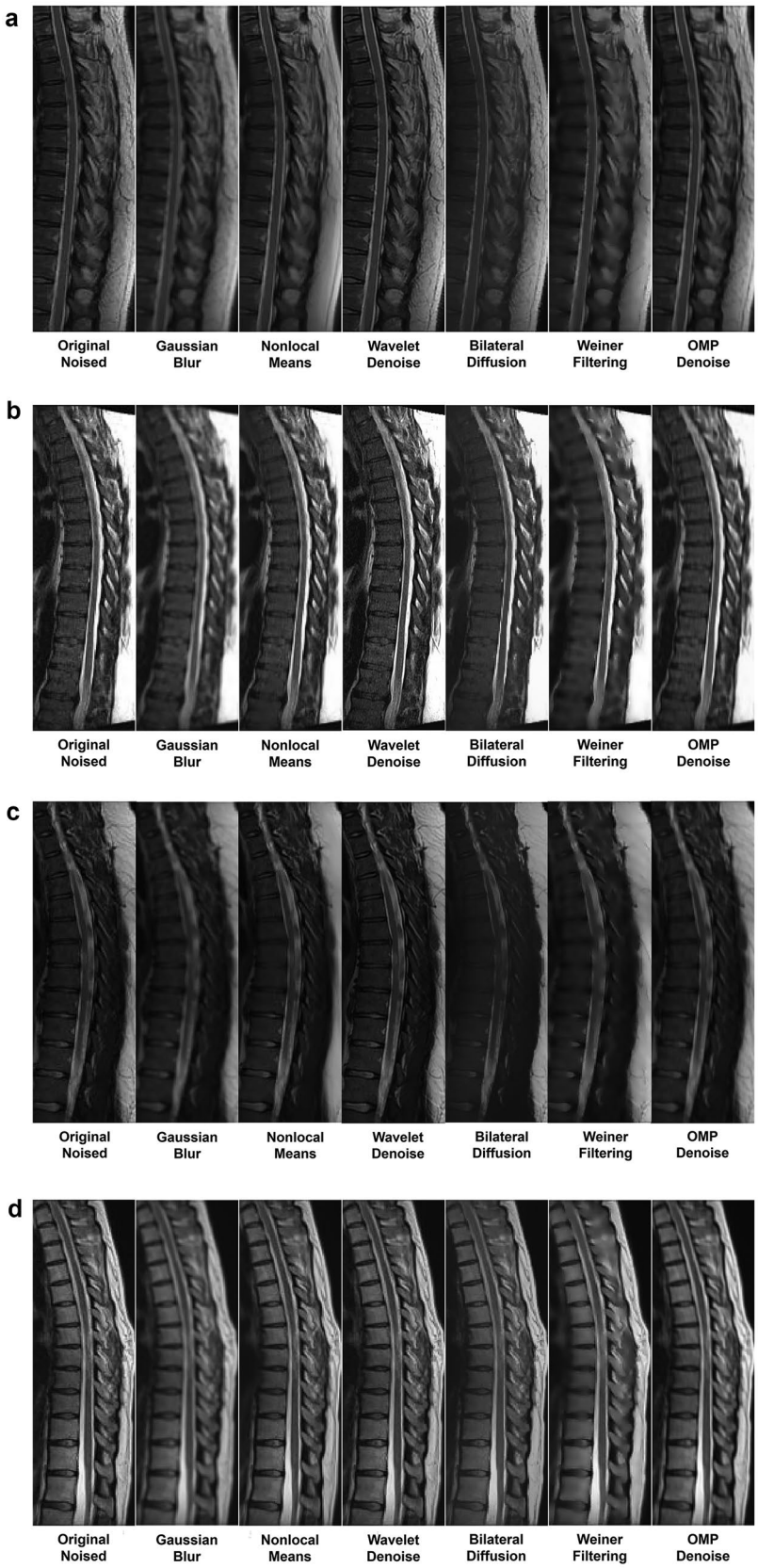


**Fig. 2** Denoising Examples with Compared Algorithms. Sagittal T2-weighted images of the thoracic spine demonstrating signal abnormalities of the spinal cord which were initially reported as artifact (a and b) versus true lesion (c and d). **a** Suspected Artifact #1, **b** Suspected Artifact #2, **c** Suspected Lesion #1, **d** Suspected Lesion #2

**Table 2** Summary performance across patient MRIs (n = 50)

| | PSNR | s.d | SSIM | s.d |
|---|---|---|---|---|
| **Gaussian blur** | 31.7 | 4.1 | 0.94 | 0.02 |
| **Nonlocal means** | 38.0 | 2.9 | 0.95 | 0.02 |
| **Wavelet** | 56.9 | 4.9 | 0.94 | 0.10 |
| **Bilateral diffusion** | 35.5 | 2.2 | 0.90 | 0.03 |
| **Weiner filter** | 34.1 | 2.7 | 0.96 | 0.02 |
| **OMP** | 37.6 | 1.7 | 0.99 | 0.01 |

Current efforts include utilization of containerizing the algorithm which has been created but not yet implemented within a PACS system. Once deployed within a clinical environment, further research in a prospective manner is planned for further characterization of not only the quantitative improvement in image quality, but the improved clinical performance and workflow optimization with resultant patient outcomes.

## Conclusion

Our study has provided a glimpse at a unique, individualized, lightweight denoising algorithm which was superior with a consistent SSIM when compared to traditional filtering mechanisms in the study. While wavelet denoising provided significant PSNR in most cases, the SSIM was widely variable which may impact consistent diagnostic accuracy. OMP denoising of medical images may provide enhanced benefits to the Neurologist and Radiologist, workflow optimization of both parties, and hopefully the improved treatment outcomes of patients who suffer from MS. Continued work within the clinical environment is underway to experimentally test the utility of this algorithm in real-world Imaging Enterprises.

**Author contribution** John Mayfield Data scientist, engineer, primary author, first draft creation. Katie Bailey Data procurement, image preprocessing, commented on manuscript revisions. Andrew Borkowski Model testing, contributing author, commented on manuscript revisions. Narayan Viswanadhan Patient identification, IRB clearance, contributing author, commented on manuscript revisions.

**Data availability** The algorithm is licensed under USF TTO: https://usf.technologypublisher.com/techcase/22A116. Contact: USF Technology Transfer. TTOinfo@usf.edu (813) 974-0994.

## Declarations

**Ethics Approval** This is an observational study. The VA Research Ethics Committee has confirmed that no ethical approval is required.

**Consent to Participate** Informed consent was waived per IRB as this was a retrospective study. Patients upon receiving any scan within the facility network sign a form stating their deidentified exams may be used for future research and teaching purposes.

**Consent for Publication** The authors affirm that informed consent was waived per the IRB for publication of the images in Figs. 1 and 2.

**Competing Interests** Financial interests: The authors have no relevant financial interest.

Non-financial interest: Dr. Mayfield has an accepted application for the algorithm to be a provisional U.S. patent as of 8/25/2022. Although currently licensed by USF, no financial compensation has been a result of this. The remaining authors have no relevant non-financial interests to disclose.

## References


1. Walton, Clare, et al. "Rising prevalence of multiple sclerosis worldwide: insights from the Atlas of MS." *Multiple Sclerosis Journal* 26.14 (2020): 1816–1821.
2. Dobson, Ruth, and Gavin Giovannoni. "Multiple sclerosis–a review." European journal of neurology 26.1 (2019): 27-40.
3. Thompson AJ, Banwell BL, Barkhof F, Carroll WM, Coetzee T, Comi G, Correale J, Fazekas F, Filippi M, Freedman MS, Fujihara K. Diagnosis of multiple sclerosis: 2017 revisions of the McDonald criteria. The Lancet Neurology. 2018 Feb 1;17(2):162-73.
4. Wattjes MP, Ciccarelli O, Reich DS, Banwell B, de Stefano N, Enzinger C, Fazekas F, Filippi M, Frederiksen J, Gasperini C, Hacohen Y. 2021 MAGNIMS–CMSC–NAIMS consensus recommendations on the use of MRI in patients with multiple sclerosis. The Lancet Neurology. 2021 Aug 1;20(8):653-70.
5. Arena L, Morehouse HT, Safir J. MR imaging artifacts that simulate disease: how to recognize and eliminate them. Radiographics. 1995 Nov;15(6):1373-94.
6. Morelli JN, Runge VM, Ai F, Attenberger U, Vu L, Schmeets SH, Nitz WR, Kirsch JE. An image-based approach to understanding the physics of MR artifacts. Radiographics. 2011 May;31(3):849-66.
7. Fazekas F, Barkhof F, Filippi M, Grossman RI, Li DK, McDonald WI, McFarland HF, Paty DW, Simon JH, Wolinsky JS, Miller DH. The contribution of magnetic resonance imaging to the diagnosis of multiple sclerosis. Neurology. 1999 Aug 1;53(3):448-.
8. Gass A, Rocca MA, Agosta F, Ciccarelli O, Chard D, Valsasina P, Brooks JC, Bischof A, Eisele P, Kappos L, Barkhof F. MRI monitoring of pathological changes in the spinal cord in patients with multiple sclerosis. The Lancet Neurology. 2015 Apr 1;14(4):443-54.
9. Kearney H, Miller DH, Ciccarelli O. Spinal cord MRI in multiple sclerosis—diagnostic, prognostic and clinical value. Nature Reviews Neurology. 2015 Jun;11(6):327-38.
10. Lycklama G, Thompson A, Filippi M, Miller D, Polman C, Fazekas F, Barkhof F. Spinal-cord MRI in multiple sclerosis. The Lancet Neurology. 2003 Sep 1;2(9):555-62.
11. Sagheer SV, George SN. A review on medical image denoising algorithms. Biomedical signal processing and control. 2020 Aug 1;61:102036.
12. Seetha J, Raja SS. Denoising of MRI images using filtering methods. In2016 International Conference on Wireless Communications, Signal Processing and Networking (WiSPNET) 2016 Mar 23 (pp. 765–769). IEEE.
13. Chandrashekar L, Sreedevi A. Assessment of non-linear filters for MRI images. In2017 Second International Conference on Electrical, Computer and Communication Technologies (ICECCT) 2017 Feb 22 (pp. 1–5). IEEE.
14. Saladi S, Amutha Prabha N. Analysis of denoising filters on MRI brain images. International Journal of Imaging Systems and Technology. 2017 Sep;27(3):201-8.
15. Chen Z, Zhou Z, Adnan S. Joint low-rank prior and difference of Gaussian filter for magnetic resonance image denoising. Medical & Biological Engineering & Computing. 2021 Mar;59:607-20.

16. Manjón JV, Carbonell-Caballero J, Lull JJ, García-Martí G, Martí-Bonmatí L, Robles M. MRI denoising using non-local means. Medical image analysis. 2008 Aug 1;12(4):514-23.
17. Jomaa H, Mabrouk R, Khlifa N, Morain-Nicolier F, Denoising of dynamic pet images using a multi-scale transform and non-local means filter, Biomed. Signal Process. Control 41 (2018) 69–80.
18. Ouahabi A. A review of wavelet denoising in medical imaging. In2013 8th International Workshop on Systems, Signal Processing and their Applications (WoSSPA) 2013 May 12 (pp. 19–26). IEEE.
19. Zhang B, Allebach JP. Adaptive bilateral filter for sharpness enhancement and noise removal. IEEE transactions on Image Processing. 2008 Mar 31;17(5):664-78.
20. Choi D, Kang SH, Park CR, Lee Y. Study of the noise reduction algorithm with median modified Wiener filter for T2-weighted magnetic resonance brain images. Journal of Magnetics. 2021 Mar;26(1):50-9.
21. Liu Y, Zhan Z, Cai JF, Guo D, Chen Z, Qu X. Projected iterative soft-thresholding algorithm for tight frames in compressed sensing magnetic resonance imaging. IEEE transactions on medical imaging. 2016 Apr 6;35(9):2130-40.
22. Izadi S, Sutton D, Hamarneh G. Image denoising in the deep learning era. Artificial Intelligence Review. 2022 Nov 15:1-46.
23. Fernández Patón M, Cerdá Alberich L, Sangüesa Nebot C, Martinez de Las Heras B, Veiga Canuto D, Cañete Nieto A, Martí-Bonmatí L. MR denoising increases radiomic biomarker precision and reproducibility in oncologic imaging. Journal of Digital Imaging. 2021 Oct;34(5):1134–45.
24. Lin DJ, Johnson PM, Knoll F, Lui YW. Artificial intelligence for MR image reconstruction: an overview for clinicians. Journal of Magnetic Resonance Imaging. 2021 Apr;53(4):1015-28.
25. Aamir F, Aslam I, Arshad M, Omer H. Accelerated diffusion-weighted MR image reconstruction using deep neural networks. Journal of Digital Imaging. 2022 Nov 4:1-3.
26. Chen Z, Pawar K, Ekanayake M, Pain C, Zhong S, Egan GF. Deep learning for image enhancement and correction in magnetic resonance imaging—state-of-the-art and challenges. Journal of Digital Imaging. 2022 Nov 2:1-27.
27. Donoho DL, Tsaig Y, Drori I, Starck JL. Sparse solution of underdetermined systems of linear equations by stagewise orthogonal matching pursuit. IEEE transactions on Information Theory. 2012 Feb 6;58(2):1094-121.
28. Fazelnia G, Paisley J. Probabilistic orthogonal matching pursuit. In 2022 IEEE International Conference on Big Data (Big Data) 2022 Dec 17 (pp. 26–35). IEEE.
29. Guo Q, Zhang C, Zhang Y, Liu H. An efficient SVD-based method for image denoising. IEEE transactions on Circuits and Systems for Video Technology. 2015 Mar 25;26(5):868-80.
30. Wang YH, Qiao J, Li JB, Fu P, Chu SC, Roddick JF. Sparse representation-based MRI super-resolution reconstruction. Measurement. 2014 Jan 1;47:946-53.
31. Tong T, Caballero J, Bhatia K, Rueckert D. Dictionary learning for medical image denoising, reconstruction, and segmentation. In Machine learning and medical imaging 2016 Jan 1 (pp. 153–181). Academic Press.
32. Liu J, Ma J, Zhang Y, Chen Y, Yang J, Shu H, Luo L, Coatrieux G, Yang W, Feng Q, Chen W. Discriminative feature representation to improve projection data inconsistency for low dose CT imaging. IEEE transactions on medical imaging. 2017 Aug 14;36(12):2499-509.
33. Leal N, Zurek E, Leal E. Non-local SVD denoising of MRI based on sparse representations. Sensors. 2020 Mar 10;20(5):1536.
34. Ravishankar S, Bresler Y. Efficient blind compressed sensing using sparsifying transforms with convergence guarantees and application to magnetic resonance imaging. SIAM Journal on Imaging Sciences. 2015;8(4):2519-57.
35. Sandino CM, Cheng JY, Chen F, Mardani M, Pauly JM, Vasanawala SS. Compressed sensing: from research to clinical practice with deep neural networks: shortening scan times for magnetic resonance imaging. IEEE signal processing magazine. 2020 Jan 17;37(1):117-27.

**Publisher's Note** Springer Nature remains neutral with regard to jurisdictional claims in published maps and institutional affiliations.

Springer Nature or its licensor (e.g. a society or other partner) holds exclusive rights to this article under a publishing agreement with the author(s) or other rightsholder(s); author self-archiving of the accepted manuscript version of this article is solely governed by the terms of such publishing agreement and applicable law.